

**SHEAR THICKENING FLUID ENCAPSULATION IN
ELECTROSPUN UHMWPE AND ITS BALLISTIC
PERFORMANCE UNDER HIGH STRAIN RATE**

PRAJESH NAYAK



**DEPARTMENT OF MATERIALS SCIENCE AND ENGINEERING
INDIAN INSTITUTE OF TECHNOLOGY DELHI
JANUARY 2023**

© Indian Institute of Technology Delhi (IITD), New Delhi, 2023

**SHEAR THICKENING FLUID ENCAPSULATION IN
ELECTROSPUN UHMWPE AND ITS BALLISTIC
PERFORMANCE UNDER HIGH STRAIN RATE**

by

PRAJESH NAYAK

Department of Materials Science and Engineering

Submitted

In fulfilment of the requirements of the degree of Doctor of Philosophy
to the



INDIAN INSTITUTE OF TECHNOLOGY DELHI

JANUARY 2023

"Mind is like water,

When it is agitated, it becomes difficult to see,

But if you allow it to settle, the answer becomes clear."


- Master Oogway

Dedicated
To My
'Family'

CERTIFICATE

This is to certify that the thesis entitled, "Shear thickening fluid encapsulation in electrospun UHMWPE and its ballistic performance under high strain rate" submitted by Ms. Prajesh Nayak to the Indian Institute of Technology Delhi, for the fulfilment of award of the degree, Doctor of Philosophy, is a record of bonafide research work carried out by her under our supervision and guidance. This thesis has been prepared in conformity with the rules and regulations of the Indian Institute of Technology Delhi, New Delhi.

The thesis, in our opinion, is worthy of consideration for award of the degree of Doctor of Philosophy in accordance with the regulations of the Institute. To the best of my knowledge, the results embodied in the thesis have not been submitted to any other University or Institute for the award of any other Degree or Diploma.



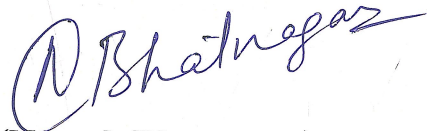
(Anup K. Ghosh)

Emeritus Professor

Department of Materials Science & Engineering

Indian Institute of Technology Delhi

Hauz Khas, New Delhi – 110016



(Naresh Bhatnagar)

Professor

Department of Mechanical Engineering

Indian Institute of Technology Delhi

Hauz Khas, New Delhi - 110016

Date- 23/1/23

Place- New Delhi

Acknowledgement

I am pleased to thank people who directly or indirectly helped me throughout this journey of completing this thesis work and making memorable days of my life at IIT Delhi.

*I express my deep gratitude to my supervisors, **Prof. Anup K. Ghosh, and Prof. Naresh Bhatnagar**, for their continuous insightful advice and guidance. I appreciate their effort and time in my personal development as a researcher by bringing the best out of me. I would like to thank them for their kind patience and trust in my abilities and for permitting freedom during the entire duration of this work.*

I am incredibly thankful to my student research committee members, Prof. Bhabani K. Satapathy, Prof. Sudip K. Pattanayek and Prof. Leena Nebhani, for their fruitful discussion and valuable suggestions that pave the way to proceed with this research work.

I am also thankful to Prof. Josemon Jacob, Prof. Sampa Saha, Prof. Bijay P. Tripathi, Prof. Rajesh Prasad, Prof. Jayant Jain, Prof. Nitya Nand Gosvami, Prof. Suresh Neelakantan, Prof. Nirat Ray, Prof. Ankur Goswami, Prof. Lakshmi Narayan Ramasubramanian., Prof. Sangeeta Santra and Prof. Shib Shankar Banerjee who made themselves available in their tight schedules for valuable discussions and support.

I would like to acknowledge the support of Mr. Tulsi Ram, Mr. Vijay Tiwari, Mr. Sanjay Singh and other Production Engineering Lab staff members, especially Mr. Anil Kumar and Mr. Prithvi Vyas, for their assistance during the completion of my experimental work.

My sincere thanks to the laboratory and office staff of DMSE, Central Research facility (CRF) and Nanoscale Research Facility (NRF), IIT Delhi, Mr. Ashok Kapoor, Mr. Surender Sharma, Mr. Ehteshamul Islam, Mr. Gajraj Singh, Mr. Jitendra Rathore, Mr. Ashish Sharma, Mr. Gyanendra Kr. Yadav, Mr. Subhash Chand, Ms. Shalini Arora, Mr. Narender Kumar, Mr. Amit Kumar, Mr. Sudhir K. Pandey, Mr. Kuldeep Sharma and Mr. Mahesh Soni, Mr. Dinesh

Sharma, Ms. Aastha Sharma and Mr. Animesh Bhowal for their kind cooperation and all possible support. Also, I thank the Department of Textile and Fiber Engineering and its laboratory staff, Dr. Vikas Khatkar and Mr. Gaurav Choudhary, for all possible help and for providing the facilities to carry out the tensile testing.

I would like to thank Prof. JSP Rai and Prof. Reena Singhal, who inspired me to pursue higher education and encouraged me during this course of research work.

I am very grateful to my seniors, juniors and colleague for their continuous endorsement and for creating joyful moments. Without them, this research work could not have been accomplished. I owe a special thanks to Dr. Hemant Chouhan and Mr. Makhan Singh for their helping hand and for providing technical support in the high strain rate testing of my samples. A special thanks to Mr. Debarghya Saha for all possible help.

I wanted to express my special thanks to Dr. Neelanchali Asija and Dr. Ranjana Nehra for their extraordinary support and encouragement throughout my doctoral studies. I sincerely appreciate my good friends Dr. Avinash Kumar, Mr. Dhruv Narayan and Mr. Makhan Singh for always helping and creating a cheerful environment.

I am thankful to Dr. Sanjay Prasad, Dr. Pankaj Chauhan, Mr. Alok Srivastava, Ms. Nisha Kumari, Ms. Aisha Ahamad, Mr. Kartikeya Shukla, Ms. Ramya Ahuja, Ms. Tarika Chadha, Mr. Khushi Ram, Mr. Rajesh Puniya, Mr. Mohit Agrawal, Mr. Madhur Pandya, Mr. Mohit Garg, Mr. Fisseha Zewdie, Mr. Ashok Bakshi, Mr. Ajit Bhagat, Mr. Mayank Prakash, Mr. Prashant Mani Shandilya and other friends for their support and making this journey incredible.

I would like to share the credit for my accomplishments with my family for always being on my side in high and low times as my source of energy in life and my carrier.

Above all, I thank 'ALMIGHTY GOD LORD KRISHNA' for his blessings and mentoring as a guru, parent and friend; you are everything. You are the one who listened and guided me

without judging me throughout this journey. I have no words to express my feeling and gratitude for you. I just want to say one thing; all things could be possible because of you.

Date- 23/01/23

Place- New Delhi

Prajesh Nayak
(Prajesh Nayak)

ABSTRACT

In this study, shear thickening fluid (STF) encapsulated electrospun ultra-high molecular weight polyethylene (UHMWPE) mat was prepared and its ballistic performance was evaluated at high strain rates under dynamic compressive loading. Two different molecular weights of UHMWPE, $M_w=2.21 \times 10^6$ g/mole (UM2.21) and 4.43×10^6 g/mole (UM4.43), were used to prepare the solutions at different concentrations in a binary mixture of decalin and cyclohexanone (70:30 ratio) solvent. Using de-Gennes's scaling theory, a correlation was established between rheological properties and electrospun morphology of the solutions to identify their critical entanglement concentrations, the concentrations at which polymer molecules started to entangle with each other. A smooth fibrous morphology was obtained when the concentration of the solution reached to 2-2.5 times the entanglement concentration. Further work was carried out by choosing higher molecular weight UHMWPE (UM4.43) at its optimum smooth fiber solution concentration (2 wt.%) due to its better properties. Other electrospinning process parameters such as applied voltage, solution conductivity, solvent type, etc were also optimized for UM4.43.

In the next step, the stretching of electrospun mat of UM4.43 was performed inside a hot air oven at different temperature range from 60-150°C. These stretched fibers, along with a single fiber of Spectra® lamina (as a control sample), were characterized for their mechanical performance and morphological analysis by SEM, XRD and tensile test under quasi-static condition.

Shear thickening fluid was synthesized with nano silica particles and characterized for its rheological behavior such as steady strain rate, dynamic strain rate and structural regeneration thixotropy test. The ballistic performance of nonwoven fabric with STF was first evaluated using a commercially available nonwoven felt of UHMWPE. This hypothesis of non-woven felt behavior was utilized in electrospun nonwoven fabric of UHMWPE.

Before STF impregnation in the electrospun mat, the surface properties such as the low coefficient of friction of UHMWPE fibers were altered by solution blending of high-density polyethylene (HDPE) with UHMWPE to increase the adhesion of silica particles on the fiber surface. Electrospinning of UHMWPE (UM4.43) and HDPE blended solution was performed at three different weight ratio compositions (100:0, 67:33 and 50:50) for obtaining miscible blend compositions. Mat prepared at miscible blends composition of UHMWPE and HDPE (67:33) was selected for shear thickening fluid impregnation study. Lastly, STF impregnated electrospun UHMWPE/HDPE fabric and UHMWPE felt (as a control sample) were encapsulated firmly by enclosing them using stretched UHMWPE fiber and tested for its high strain rate behavior. The high strain rate performance of STF encapsulated samples showed a significant improvement in peak stress in both samples enclosed by stretched UHMWPE fiber as compared to the unenclosed neat felt sample. From this study it was found that STF encapsulation after its impregnation in the fabric can improve the ballistic performance by helping STF to perform synergistically with lab synthesised electrospun fabric and can be a precursor for further technology development.

सार

इस अध्ययन में, शीयर थिकनिंग फ्लुइड (एसटीएफ) एनकैप्सुलेटेड इलेक्ट्रोस्पुन अल्ट्रा-हाई मॉलिक्यूलर वेट पॉलीइथाइलीन (यूएचएमडब्ल्यूपीई) मैट तैयार किया गया था और डायनेमिक कंप्रेसिव लोडिंग के तहत उच्च तनाव दरों पर इसके बैलिस्टिक प्रदर्शन का मूल्यांकन किया गया था। यूएचएमडब्ल्यूपीई के दो अलग-अलग आणविक भार, $M_w=2.21 \times 10^6$ (यूएम2.21) और 4.43×10^6 ग्राम/मोल (यूएम4.43), का उपयोग डेकालिन और साइक्लोहेक्सानोन के द्विआधारी मिश्रण में विभिन्न सांद्रता पर समाधान तैयार करने के लिए किया गया था। (70:30 अनुपात) विलायक। डी-जीन्स के स्केलिंग सिद्धांत का उपयोग करते हुए, उनके महत्वपूर्ण उलझाव सांद्रता की पहचान करने के लिए समाधानों के रियोलॉजिकल गुणों और इलेक्ट्रोस्पन आकारिकी के बीच एक सहसंबंध स्थापित किया गया था, जिस सांद्रता पर बहुलक अणु एक दूसरे के साथ उलझने लगे थे। एक चिकनी रेशेदार आकृति विज्ञान प्राप्त किया गया था जब समाधान की एकाग्रता उलझाव की एकाग्रता के 2-2.5 गुना तक पहुंच गई थी। इसके बेहतर गुणों के कारण इष्टतम चिकनी फाइबर समाधान एकाग्रता (2 wt%) पर उच्च आणविक भार यूएचएमडब्ल्यूपीई (यूएम4.43) को चुनकर आगे का काम किया गया। अन्य इलेक्ट्रोस्पनिंग प्रक्रिया पैरामीटर जैसे लागू वोल्टेज, समाधान चालकता, विलायक प्रकार, आदि को भी यूएम4.43 के लिए अनुकूलित किया गया था।

अगले चरण में, यूएम4.43 के इलेक्ट्रोस्पन मैट को 60-150 °C से अलग तापमान रेंज में गर्म हवा के ओवन के अंदर खींचा गया था। स्पेक्ट्रा® लेमिना (एक नियंत्रण नमूने के रूप में) के एक एकल फाइबर के साथ इन फैले हुए तंतुओं को अर्ध-स्थैतिक स्थिति के तहत एसईएम, एक्सआरडी और तन्यता परीक्षण द्वारा उनके यांत्रिक प्रदर्शन और रूपात्मक विश्लेषण के लिए चित्रित किया गया था।

कतरनी गाढ़ा द्रव नैनो सिलिका कणों के साथ संश्लेषित किया गया था और इसके रियोलॉजिकल व्यवहार जैसे स्थिर तनाव दर, गतिशील तनाव दर और संरचनात्मक पुनर्जनन थिक्सोट्रॉपी परीक्षण के लिए विशेषता थी। एसटीएफ के साथ गैर बुने हुए कपड़े के बैलिस्टिक प्रदर्शन का मूल्यांकन पहले यूएचएमडब्ल्यूपीई

के व्यावसायिक रूप से उपलब्ध गैर बुने हुए महसूस का उपयोग करके किया गया था। गैर बुने हुए महसूस किए गए व्यवहार की इस परिकल्पना का उपयोग यूएचएमडब्ल्यूपीई के इलेक्ट्रोस्पन गैर बुने हुए कपड़े में किया गया था।

इलेक्ट्रोस्पन मैट में एसटीएफ संसेचन से पहले, यूएचएमडब्ल्यूपीई फाइबर के घर्षण के कम गुणांक जैसे सतह गुणों को फाइबर सतह पर सिलिका कणों के आसंजन को बढ़ाने के लिए यूएचएमडब्ल्यूपीई के साथ उच्च घनत्व पॉलीथीन (एचडीपीई) के मिश्रण से बदल दिया गया था। यूएचएमडब्ल्यूपीई (यूएम4.43) और एचडीपीई ब्लेंडेड सॉल्यूशन की इलेक्ट्रोस्पनिंग तीन अलग-अलग वेट रेशियो कंपोज़िशन (100:0, 67:33 और 50:50) पर की गई थी ताकि मिसिबल ब्लेंड कंपोज़िशन प्राप्त किया जा सके। यूएचएमडब्ल्यूपीई और एचडीपीई (67:33) के गलत मिश्रण मिश्रण पर तैयार चटाई को कतरनी गाढ़ा द्रव संसेचन अध्ययन के लिए चुना गया था। अंत में, एसटीएफ ने इलेक्ट्रोस्पन यूएचएमडब्ल्यूपीई/एचडीपीई फैब्रिक और यूएचएमडब्ल्यूपीई महसूस किया (एक नियंत्रण नमूने के रूप में) उन्हें फैलाए गए यूएचएमडब्ल्यूपीई फाइबर का उपयोग करके मजबूती से घेर लिया गया और इसके उच्च तनाव दर व्यवहार के लिए परीक्षण किया गया। एसटीएफ एनकैप्सुलेटेड नमूनों के उच्च तनाव दर प्रदर्शन ने यूएचएमडब्ल्यूपीई फाइबर से घिरे दोनों नमूनों में बिना साफ-सुथरे महसूस किए गए नमूने की तुलना में चरम तनाव में महत्वपूर्ण सुधार दिखाया। इस अध्ययन से यह पाया गया कि कपड़े में संसेचन के बाद एसटीएफ एनकैप्सुलेशन, एसटीएफ को प्रयोगशाला संश्लेषित इलेक्ट्रोस्पन कपड़े के साथ सहक्रियात्मक रूप से प्रदर्शन करने में मदद करके बैलिस्टिक प्रदर्शन में सुधार कर सकता है और आगे के प्रौद्योगिकी विकास के लिए अग्रदूत साबित हो सकता है।

Table of Contents

Certificate.....	I
Acknowledgement	III
Abstract	VII
Table of Contents	XI
List of Figures	XVII
List of Tables	XXV
List of Abbreviations	XXVII
List of Symbols	XXIX
Preamble	1
CHAPTER 1: INTRODUCTION AND LITERATURE REVIEW	7
1.1 Introduction of ultra-fine fibers manufacturing	7
1.2 Nanofibers formation methods.....	7
1.2.1 Drawing method	7
1.2.2 Phase separation	7
1.2.3 Template synthesis	7
1.2.4 Self-assembly.....	8
1.2.5 Electrospinning process	8
1.2.5.1 Melt electrospinning process	8
1.2.5.2 Solution electrospinning process	9
1.3 Brief background of electrospinning.....	10
1.4 Fundamentals of fiber formation by electrospinning	11
1.5 Parameters affecting solution electrospinning process	14
1.5.1 Literature review on process parameters	15
1.5.1.1 Solution parameters	15
1.5.1.1.1 Effect of polymer concentration on fiber morphology.....	15
1.5.1.1.2 Effect of polymer molecular weight.....	17
1.5.1.1.3 Effect of solution viscosity.....	18
1.5.1.1.4 Effect of conductivity	19
1.5.1.1.5 Effect of surface tension.....	20
1.5.1.2 Process parameters.....	20
1.5.1.2.1 Effect of applied voltage	20

1.5.1.2.2 Effect of flow rate	21
1.5.1.2.3 Effect of collector	22
1.5.1.2.4 Effect of the needle tip to collector distance (NCD)	23
1.5.1.2.5 Effect of the needle gauge	23
1.5.1.3 Ambient parameters	24
1.5.1.3.1 Effect of temperature and humidity	24
1.6 Modelling of electrospinning process	25
1.6.1 Jet initiation and their elongation	25
1.6.2 Thinning of jet	26
1.6.3 Jet solidification	27
1.7 Ultra-high molecular weight polyethylene	28
1.8 Literature review on high-temperature electrospinning of polyolefins	30
1.9 Shear thickening fluid	36
1.9.1 Theory of shear thickening mechanism	37
1.9.1.1 Order-disorder transition (ODT)	37
1.9.1.2 Hydrocluster mechanism	37
1.9.2 Parameters affecting the shear thickening phenomenon	39
1.9.3 Literature review on application of STF in ballistic clothing	40
1.10 High strain rate testing	41
1.10.1 Assumptions for SHPB testing	43
1.10.2 Background and history of Split-Hopkinson pressure bar	43
1.10.3 Application of SHPB	44
1.11 Literature outcomes & gaps	45
1.12 Objective of the work	46
1.13 Plan of work	46
CHAPTER 2: MATERIALS AND EXPERIMENTAL METHOD	51
2.1 Raw materials	51
2.1.1 Ultra-high molecular weight polyethylene (UHMWPE)	52
2.1.1.1 Morphology of UHMWPE powder by SEM analysis	52
2.1.1.2 Wide-angle X-ray diffraction analysis (WAXD)	53
2.1.1.3 Thermal analysis	54
2.1.1.4 FTIR analysis	57
2.1.2 High-Density Polyethylene (HDPE)	58

2.1.2.1 Thermal Analysis	58
2.1.3 UHMWPE felt	59
2.1.3.1 Morphology of felt	60
2.1.3.2 Thermal analysis of felt fibers	60
2.1.3.3 FTIR analysis of felt	61
2.1.3.4 Wide-angle X-ray analysis of felt fibers	62
2.2 Experimental techniques	62
2.2.1 High-temperature electrospinning method	62
2.2.2 Sonicator and hot air oven	64
2.3 Characterization techniques	66
2.3.1 Simultaneous thermal analysis (STA)	67
2.3.2 Scanning electron microscopy (SEM)	68
2.3.3 Atomic force microscopic (AFM)	69
2.3.4 Rheometer	69
2.3.5 Wide-angle X-ray diffraction	71
2.3.6 Fourier transformed infrared spectroscopy (FTIR)	71
2.3.7 Zeta potential analyzer and dynamic light scattering (DLS)	72
2.3.8 Capillary flow porometer	73
2.3.9 Tensile strength	74
2.3.10 Split-Hopkinson pressure bar	75
CHAPTER 3: PREPARATION AND CHARACTERIZATION OF ELECTROSPUN MATS OF UHMWPE FIBERS	79
3.1 Introduction	79
3.2 Sample Preparation	79
3.2.1 Preparation of UHMWPE solutions for the analysis of fiber formability	79
3.2.2 Preparation of UHMWPE mat	80
3.3 Results and discussions	81
3.3.1 Analysis of Flow Curves	81
3.3.2 Entanglement concentration of UHMWPE solution	83
3.3.2.1 Effect of entanglement concentration on the fiber morphology	85
3.3.3 Effect of applied voltage on fiber morphology	93
3.3.4 Effect of solution conductivity	94
3.3.5 Effect of solvent types	96
3.3.6 Mechanical properties	98

3.3.7 Wide-angle X-ray diffraction (WAXD) analysis	100
3.3.8 Post-processing treatment of electrospun mat of UHMWPE.....	101
3.3.8.1 High temperature stretching of the mat	102
3.3.8.2 Effect of temperature on draw ratio	103
3.3.8.2.1 Surface morphology of fiber	105
3.3.8.2.2 Structure analysis by WAXD	107
3.3.8.2.3 Performance evaluation.....	109
3.3.8.2.4 Fractographic analysis.....	112
3.4 Summary	113
CHAPTER 4: PREPARATION AND CHARACTERIZATION OF SHEAR THICKENING FLUID.....	117
4.1 Morphological analysis of silica nanoparticles	117
4.2 Zeta potential of silica nanoparticles.....	118
4.3 Particle size and distribution	118
4.4 Shear thickening fluid preparation by the ultra-sonication method.....	119
4.5 Thermogravimetric analysis of STF.....	120
4.6 Rheological properties of STF	121
4.6.1 Dilatant behavior of STF	121
4.6.2 Oscillatory test of STF.....	122
4.6.2.1 Amplitude sweep	122
4.6.2.2 Frequency sweep.....	123
4.6.3 Thixotropic behavior of STF	124
4.7 Summary	125
CHAPTER 5: ELECTROSPINNING OF UHMWPE/HDPE BLENDS AND THEIR CHARACTERIZATION	129
5.1 Introduction	129
5.2 Solution preparation and electrospinning of UHMWPE and HDPE blended fibers....	129
5.3 Results and discussions	130
5.3.1 Rheological analysis of the UHMWPE and HDPE blended solutions.....	130
5.3.2 Morphological analysis of fiber.....	131
5.3.2.1 Surface morphology	131
5.3.2.2 Fiber surface topography	134
5.3.2.3 Wide-angle X-ray diffraction (WAXD) analysis.....	136
5.3.3 Porosity and pore size analysis of mats	137

5.3.4 Thermal analysis.....	140
5.3.4.1 DSC analysis.....	140
5.3.4.2 Thermogravimetric analysis (TGA).....	141
5.3.5 Mechanical analysis.....	142
5.4 Summary	144
CHAPTER 6: IMPREGNATION OF UHMWPE WITH SHEAR THICKENING FLUID FOR BALLISTIC APPLICATIONS	149
6.1 Introduction	149
6.2 Preparation of sample for SHPB testing	150
6.2.1 Soaking of nonwoven UHMWPE felt with STF	150
6.3 High strain rate testing by SHPB	151
6.3.1 Split-Hopkinson pressure bar methodology	152
6.4 Results and discussions	156
6.4.1 Morphological analysis of STF impregnated felt	156
6.4.2 High strain rate testing of STF treated felt by SHPB	157
6.4.3 Microstructural analysis of samples	162
6.5 Summary	164
CHAPTER 7: MECHANICAL BEHAVIOR OF SHEAR THICKENING FLUID ENCAPSULATED UHMWPE FOR HIGH STRAIN RATE APPLICATION	169
7.1 Introduction	169
7.2 Samples preparation for SHPB testing.....	169
7.3 Background theory and mechanism of SHPB.....	170
7.4 Surface morphology and STF add-on% of STF impregnated UHMWPE/HDPE mat	171
7.5 SHPB Setup calibration.....	172
7.6 SHPB test results.....	173
7.7 Failure analysis of the electrospun sample.....	178
7.8 Summary	181
CHAPTER 8: SUMMARY, CONCLUSION AND FUTURE SCOPE.....	185
8.1 Introduction	185
8.2 Summary	185
8.3 Conclusions	186
8.4 Recommendations for future study	187
References.....	189

List of Figures

CHAPTER 1: INTRODUCTION AND LITERATURE REVIEW

Figure 1.1: Schematic diagram of electrospinning method [15]	9
Figure 1.2: Polymer chain conformation in solution: (i) dilute, (ii) semi dilute unentangled and (iii) semi dilute entangled regime	12
Figure 1.3: SEM images of electrospun products at different concentrations ranging from low to high solution concentration for producing poly(vinyl pyrrolidone) (PVP) nanofibers [41] 15	
Figure 1.4: (a) Linear long molecular chain and (b) Lamella structure of UHMWPE [106].	29
Figure 1.5: Schematic of the electrostatic spinning apparatus [91]	31
Figure 1.6: Electrospinning device used for UHMWPE fiber [125]	35
Figure 1.7: The log-log plot of viscosity vs. shear rate of shear thickening suspension [129]	36
Figure 1.8: (a) At low Péclet number, Brownian motion caused perikinetic aggregation of particles and (b) at high Péclet number, hydrodynamic interactions caused orthokinetic aggregation of particles [135]	38
Figure 1.9: Flow chart representing detailed thesis work plan	47

CHAPTER 2: MATERIALS AND EXPERIMENTAL METHOD

Figure 2.1: (a) UHMWPE powder of UM2.21 and (b)-(d) its SEM images at different magnifications of 55×, 500× and 2500× respectively	52
Figure 2.2: (a) UHMWPE powder of UM4.43 and (b)-(d) its SEM images at different magnification of 500×, 10K× and 50K× respectively	53
Figure 2.3: Wide-angle X-ray diffraction patterns of (a) UM2.21 and (b) UM4.43 powder .	54
Figure 2.4: (a) DSC and (b) TGA analysis of UM2.21 powder	54
Figure 2.5: (a) DSC and (b) TGA scan of UM4.43 powder	55
Figure 2.6: FTIR spectra of UM2.21 powder	57
Figure 2.7: FTIR spectra of UM4.43 powder	58
Figure 2.8: (a) DSC and (b) TGA scan curves of HDPE.....	58
Figure 2.9: Surface morphology of UHMWPE felt fibers at a magnification of (a) 100× and (b) 500×	60
Figure 2.10: (a) DSC and (b) TGA thermograms of UHMWPE felt fibers	61

Figure 2.11: FTIR analysis of UHMWPE felt fibers.....	61
Figure 2.12: XRD pattern of UHMWPE felt fibers.....	62
Figure 2.13: Typical electrospinning setup consisting of the heating assembly shown by an enlarged image	63
Figure 2.14: Ultrasonic homogenizer set-up.....	64
Figure 2.15: Hot air oven to evaporate excess ethanol from suspension to make STF	65
Figure 2.16: Perkin-Elmer STA 6000 simultaneous thermal analyzer instrument.....	67
Figure 2.17: Zeiss EVO 18 Special Model, scanning electron microscopy	68
Figure 2.18: Asylum Research MFP3D-BIO atomic force microscope	69
Figure 2.19: (a) MCR 702 TwinDrive Anton Paar advanced rheometer, (b) cub and bob and (c) cone and plate measuring systems.....	70
Figure 2.20: Rigaku Ultima IV WAXD instrument	71
Figure 2.21: Thermo Scientific, Nicolet iS50 spectrometer instrument	72
Figure 2.22: Malvern Zetasizer Nano-ZS instrument.....	72
Figure 2.23: POROLUX™ 100NW capillary flow porometer.....	73
Figure 2.24: Universal testing machine, Instron 3365 model.....	74
Figure 2.25: In-house designed SHPB setup having (a) Ti alloy bars and (b) maraging steel bars.....	75

CHAPTER 3: PREPARATION AND CHARACTERIZATION OF ELECTROSPUN MATS OF UHMWPE FIBERS

Figure 3.1: Illustration of the schematic diagram of the experimental process of solutions such as their rheological testing and electrospinning.....	80
Figure 3.2: Viscosity vs. shear rate curve of UM2.21 solutions at 130°C for different concentrations	81
Figure 3.3: Viscosity vs. shear rate curve of UM4.43 solutions at 130°C for different concentrations	82
Figure 3.4: Plot of specific viscosity (η_{sp}) vs. concentration for (a) UM2.21 and (b) UM4.43 solutions	83
Figure 3.5: Calculated entanglement number ($n_{e,sol}$) vs. concentration for the UHMWPE / (decalin : cyclohexanone) system.	85
Figure 3.6: SEM images for electrospun product (with electrospinning parameters: flow rate 1 μ l/sec, voltage 15 kV and 20 cm distance from needle tip to collector) for UM2.21 at (a) 0.5	

wt.%, (b)1.0 wt.%, (c) 1.5 wt.%, (d) 2.0 wt.%, (e) 2.5 wt.%, (f), 3. 0 wt.%, (g) 3.5 wt.% and (h) 4.0 wt.% concentrations	86
Figure 3.7: Fiber diameter distribution of UM2.21 electrospun fibers at (a) 1.5 wt.%, (b) 2 wt.%, (c) 2.5 wt.%, (d) 3 wt.%, (e) 3.5 wt.% and (f) 4 wt.% concentration.....	87
Figure 3.8: Viscosity (zero shear viscosity) vs. average fiber diameter relation for UM2.21 and UM4.43 solutions.....	88
Figure 3.9: SEM images for electrospun product (with electrospinning parameters: flow rate 1 μ l/sec, voltage 15 kV and 20 cm distance from needle tip to collector) for UM4.43 solutions at (a) 0.1 wt.%, (b) 0.5 wt.%, (c) 1.0 wt.%, (d) 1.5 wt.%, (e) 2.0 wt. and (f) 2.5 wt.% concentration.....	89
Figure 3.10: Fiber diameter distribution of UM4.43 electrospun fibers at different solution concentrations: (a) 0.5 wt.%, (b) 1 wt.%, (c) 1.5 wt.%, (d) 2 wt.% and (e) 2.5 wt.%	90
Figure 3.11: Correlation of average fiber diameter with normalized concentration for UM2.21 and UM4.43 solutions	91
Figure 3.12: SEM micrographs from UM4.43M in a binary mixture of decalin/cyclohexanone (70:30) in different concentrations: (a) 0.1%, (b) 0.5 %, (c) 1%, (d) 1.5% (e) 2 % and (f) 2.5% wt.% at 25kV applied voltage.....	93
Figure 3.13: Average fiber diameter versus polymer concentration of UM4.43 dissolved in decalin: cyclohexanone (70:30) at two different voltages of 15 kV and 25 kV	94
Figure 3.14: SEM micrographs from UM4.43 at 2 wt.% concentration dissolved in a binary mixture of decalin/cyclohexanone in different concentrations: (a) 90:10, (b) 80:20, (c) 70:30, (d) 60:40 and (e) 50:50 at 15kV.....	95
Figure 3.15: Average fiber diameter vs solvent ratio of decalin: cyclohexanone at 90:10, 80:20, 70:30, 60:40 and 50:50	96
Figure 3.16: SEM micrographs from UM4.43M at 2 wt.% concentration in mixture of different solvent systems such as (a) decalin/p-xylene/cyclohexanone (50:30:20) (v/v), (b) p-xylene/decalin/cyclohexanone (50:30:20) (v/v), (c) p-xylene/cyclohexanone (70:30) (v/v), (d) p-cymene/cyclohexanone (70:30) (v/v) and (e) decalin/cyclohexanone (70:30) (v/v), at 15kV	97
Figure 3.17: Stress-strain curves of the electrospun UM4.43 mat prepared from a binary mixture of decalin/cyclohexanone at 50:50 and 70:30 ratio.....	98
Figure 3.18: Stress-strain curves of the electrospun UM4.43 mat prepared at 1.5 wt.% and 2.0 wt.% concentration in a binary mixture of decalin/cyclohexanone at a 70:30 ratio.....	99

Figure 3.19: WAXD pattern of the electrospun UM4.43 mat prepared at 1.5 wt.% concentration in a binary mixture of decalin/cyclohexanone at 50:50 and 70:30 ratio	100
Figure 3.20: WAXD pattern of the electrospun UM4.43 mat prepared at 1.5 wt.% and 2 wt.% concentration in a binary mixture of decalin: cyclohexanone at 70:30 ratio	101
Figure 3.21: Schematic diagram of the electrospinning process followed by structural evolution of structure shish kebab to highly extended chain structure due to post-processing treatment of electrospun mat.....	102
Figure 3.22: Schematic diagrams for stretching of electrospun UHMWPE fibers at a high temperature inside a hot air oven	103
Figure 3.23: Draw ratio vs. temperature of UHMWPE electrospun mat stretched at different temperature	104
Figure 3.24: Stretched UHMWPE mat strip at 130°C	105
Figure 3.25: SEM images of as-spun electrospun mat of UHMWPE at a magnification of (a) 100× and (a') 500×; mat drawn at 120°C of temperature at (b) 100× and (b') 1000×; mat drawn at 130°C at (c) 100× and (c') 500×; Spectra® fiber at (d) 100× and (d') 500× of magnification	106
Figure 3.26: XRD pattern of electrospun fibers namely (a) as spun and drawn fibers at different temperature of 90°C, 120°C, 130°C, 140°C and 150°C, (b) single fibers of different grades of Spectra®3124, Spectra®5143, Spectra®5358 and Spectra®6472.....	108
Figure 3.27: Stress vs. strain response of single fibers of different grades of Spectra® and high temperature stretched electrospun UHMWPE fibers.....	109
Figure 3.28: Stress-strain properties of as-spun and stretched yarn fibers at a temperature of 90°C, 120°C, 130°C, 140°C and 150°C and single fibers of Spectra®3124, Spectra®5143, Spectra®5358 and Spectra®6472.....	111
Figure 3.29: Tensile fracture end electrospun yarns samples stretched at (a) 120 °C and (b) 130 °C of stretching temperature and single fibers of different grades of Spectra® (c) Spectra®5143 and (d) Spectra®6472 tested at a rate of 5 mm/min at a room temperature..	112

CHAPTER 4: PREPARATION AND CHARACTERIZATION OF SHEAR THICKENING FLUID

Figure 4.1: (a) SEM morphology (b) histogram for the particles size distribution of silica nanoparticles	117
Figure 4.2: Zeta potential of silica nanoparticles.....	118

Figure 4.3: Intensity vs. particles size measurements by DLS method of silica nanoparticles in DI water	119
Figure 4.4: Thermogravimetric graph of silica suspension in PPG400.....	120
Figure 4.5: Viscosity vs. shear rate curve of shear thickening fluid.....	121
Figure 4.6: Strain amplitude sweep of STF at a constant angular frequency of 10 rad/s with varying strain from 0.001 to 100%	122
Figure 4.7: Frequency sweep of STF within the LVR range ($\gamma=1$) at a varying frequency range from 0.1 to 100 rad/s.....	123
Figure 4.8: Three intervals rotational test (3ITT) of shear thickening fluid at low shear phase $\gamma = 0.1 \text{ s}^{-1}$, $t = 450 \text{ s}$, high shear phases are $\gamma = 1000 \text{ s}^{-1}$, 2000 s^{-1} and 3000 s^{-1} , $t = 450 \text{ s}$ and low shear phase $\gamma = 0.1 \text{ s}^{-1}$, $t = 1800 \text{ s}$	124

CHAPTER 5: ELECTROSPINNING OF UHMWPE/HDPE BLENDS AND THEIR CHARACTERIZATION

Figure 5.1: Electrospun mat of UHMWPE and HDPE blended solution (UMHD1).....	130
Figure 5.2: (a) Shear stress vs. shear rate and (b) viscosity vs. shear rate curve of UMHD0, UMHD1 and UMHD2 solution	131
Figure 5.3: SEM images and histogram for the fiber size distribution of electrospun fiber of (a, a') UMHD0, (b,b') UMHD1 and (c,c') UMHD2 fibers.....	133
Figure 5.4: (a) electrospinning of UHMWPE solutions and (b) magnifying image of jet solution.....	134
Figure 5.5: AFM images (a), (a') and (a'') of electrospun fibers UMHD0, (b), (b') and (b'') of UMHD1 and (c), (c') and (c'') of UMHD2 depicted in 3D, 2D and their corresponding height images respectively	135
Figure 5.6: WAXD patterns of UMHD0, UMHD1 and UMHD2.....	137
Figure 5.7: Typical capillary flow porometry result of electrospun UMHD0 mat sample ..	138
Figure 5.8: Pore size distribution in (a) UMHD0, (b) UMHD1 and (c) UMHD2 electrospun mat samples.....	139
Figure 5.9: DSC scans of second heating (a) melting endotherm and (b) exotherm of UMHD0, UMHD1 and UMHD2 samples	140
Figure 5.10: TGA analysis of electrospun fibers of UMHD0, UMHD1 and UMHD2	141
Figure 5.11: Stress-strain plot of electrospun mat of UMHD0, UMHD1 and UMHD2 fiber samples.....	143

CHAPTER 6: IMPREGNATION OF UHMWPE WITH SHEAR THICKENING FLUID FOR BALLISTIC APPLICATIONS

Figure 6.1: Sample preparation for SHPB testing	150
Figure 6.2: Schematic diagram of Split-Hopkinson Pressure Bar setup.....	152
Figure 6.3: Lagrange diagram for wave propagation in compressive split-Hopkinson bar .	153
Figure 6.4: Schematic diagram of incident bar, sample and the transmission bar of Split-Hopkinson Pressure Bar setup	154
Figure 6.5: SEM morphology of STF impregnated UHMWPE felt fibers at a magnification of (a) 100× (b) 2.50 K× and (c) 50 K×	157
Figure 6.6: Calibration of SHPB bars (a) wave signal without reflected wave and (b) Force-time plot	157
Figure 6.7: Processing of data (a) voltage vs. time and (b) strain vs. time obtained from SHPB test results.....	159
Figure 6.8: Stress-strain plot of (a) neat UHMWPE felt and (b) STF impregnated felt deduced from SHPB test results.....	160
Figure 6.9: Impact toughness variation with strain rate for neat UHMWPE felt and STF impregnated felt	161
Figure 6.10: Images of (a) neat felt tested at a strain rate of (b) 11000 s ⁻¹ (c) 11500 s ⁻¹ and (d) STF impregnated felt tested at a strain rate of (e) 13350 s ⁻¹ (f) 15500 s ⁻¹	163
Figure 6.11: SEM images of (a) neat felt impacted at a strain rate of (b) 11500 s ⁻¹ and (c) STF impregnated felt impacted sample at a strain rate of (d) 15500 s ⁻¹	164

CHAPTER 7: MECHANICAL BEHAVIOR OF SHEAR THICKENING FLUID ENCAPSULATED UHMWPE FOR HIGH STRAIN RATE APPLICATION

Figure 7.1: Neat felt sample mounted between the incident and transmitter bars of SHPB setup	171
Figure 7.2: SEM images of (a)-(b) neat UHMWPE/HDPE mat fibers and (c)-(d) STF impregnated UHMWPE-HDPE mat fibers, at a magnification of 100× and 5K×, respectively	172
Figure 7.3: Force-time plot for calibration of Split-Hopkinson pressure bar (C-250 maraging steel).....	173
Figure 7.4: Dynamic stress-strain plot of neat and STF encapsulated samples of (a),(b) electrospun mat and (c),(d) felt samples	174

Figure 7.5: Peak stress vs. strain rate of neat and STF encapsulated electrospun and felt samples.....176

Figure 7.6: Toughness variation with a strain rate of neat and STF encapsulated electrospun and felt sample177

Figure 7.7: Deformation of the neat electrospun sample at high strain rate loading of 6837 s^{-1} 179

Figure 7.8: Analysis for deformation of STF encapsulated electrospun sample at high strain rate loading of 3974 s^{-1} 180

Figure 7.9: Photographic and SEM images of high strain rate tested (a)(a') neat and (b)(b') STF encapsulated electrospun sample at 6837 s^{-1} and 3974 s^{-1} of strain rate.....181

List of Tables

CHAPTER 1: INTRODUCTION AND LITERATURE REVIEW

Table 1.1: Electrospinning parameters..... 14

Table 1.2: Testing methods with their associated strain rate ranges and conditions42

CHAPTER 2: MATERIALS AND EXPERIMENTAL METHOD

Table 2.1: Raw Materials, their grades and supplier's name51

Table 2.2: List of solvents used in the electrospinning process.....51

Table 2.3: DSC of UM2.21 after a common thermal history at a thermal scan of 10 °C/min 55

Table 2.4: DSC of UM4.43 sample after a common thermal history56

Table 2.5: Thermal stability parameters of UM2.21 and UM4.43 at a heating rate of 20 °C/min
.....56

Table 2.6: DSC characterization of HDPE granules sample after a common thermal history
.....59

Table 2.7: Thermal stability parameters of HDPE granules at a heating rate of 40 °C/min...59

Table 2.8: Properties of UHMWPE felt sample60

Table 2.9: List of used characterizations techniques66

Table 2.10: Specification of in-house designed SHPB setup.....76

CHAPTER 3: PREPARATION AND CHARACTERIZATION OF ELECTROSPUN MATS OF UHMWPE FIBERS

Table 3.1: Properties of UHMWPE solutions for fiber formation and average fiber diameters of UM2.21 and UM4.43.....92

Table 3.2: Properties of electrospun UHMWPE fibers: as spun, hot stretched and Spectra single fiber from XRD108

Table 3.3: Stress-strain properties of as spun, stretched electrospun yarn at 90°C, 120°C, 130°C, 140°C and 150°C along with Spectra®3124, Spectra®5143, Spectra®5358 and Spectra®6472 single fibers.....110

CHAPTER 5: ELECTROSPINNING OF UHMWPE/HDPE BLENDS AND THEIR CHARACTERIZATION

Table 5.1: Arithmetic mean roughness Ra, RMS roughness Rq and productivity of electrospun Fibers.....136

Table 5.2: Summarized results obtained from the porometry for UMHD0, UMHD1 and UMHD2 mat samples 139

Table 5.3: TGA results of UMHD0, UMHD1 and UMHD2 fibers 142

Table 5.4: Mechanical properties of electrospun of UMHD0, UMHD1 and UMHD2 144

CHAPTER 6: IMPREGNATION OF UHMWPE WITH SHEAR THICKENING FLUID FOR BALLISTIC APPLICATIONS

Table 6.1: Details of neat and STF treated UHMWPE felt sample. 151

Table 6.2: Neat and STF impregnated felt sample results by SHPB testing. 162

CHAPTER 7: MECHANICAL BEHAVIOR OF SHEAR THICKENING FLUID ENCAPSULATED UHMWPE FOR HIGH STRAIN RATE APPLICATION

Table 7.1: Neat and STF encapsulated electrospun mat and felt samples results of SHPB testing 175

List of Abbreviations

Abbreviation	Description
AFM	Atomic force microscopic
CA	Cellulose Acetate
CNT	Carbon nanotube
DLS	Dynamic light scattering
DMAC	N, N-dimethylacetamide
DMF	N, N-dimethylformamide
DSC	Differential scanning calorimetry
EG	Ethylene glycol
FTIR	Fourier transform infrared spectroscopy
HDPE	High-Density Polyethylene
HMPP	High modulus polypropylene
iPP	Isotactic polypropylene
IR	Infrared
LLDPE	Linear low-density polyethylene
LVR	Linear viscoelastic region
NCD	Needle tip to collector distance
o-DCB	O-dichlorobenzene
PAN	Polyacrylonitrile
PCL	Polycaprolactone
PDLA	Poly(d-lactic acid)
PDLLA	D,L-poly(lactic acid)
PEG	Polyethylene glycol
PEO	Polyethylene oxide
PMMA	Poly(methyl methacrylate)
PP	Polypropylene
PPG	Polypropylene glycol
PSF	Polysulfone
PUU	Polyurethane urea
PVA	Polyvinyl alcohol
PVC	Poly (Vinyl Chloride)

PVDF	Polyvinylidene fluoride
PVP	Poly(vinylpyrrolidone)
RMS	Root mean square
SD	Standard Deviation
SEM	Scanning electron microscopy
SHB	Split-Hopkinson Bar
SHPB	Split-Hopkinson Pressure Bar
SQ	Sodium oleate
STA	Simultaneous thermal analysis
STF	Shear thinning fluid
STG	Shear thickening gel
TGA	Thermogravimetric analysis
THF	Tetrahydrofuran
UHMWPE	Ultra-high molecular weight polyethylene
UM2.21	UHMWPE of 2.21 million g/mole molecular weight
UM4.43	UHMWPE of 4.43 million g/mole molecular weight
UMHD0	Neat UHMWPE (100:0)
UMHD1	UHMWPE/HDPE (67:33)
UMHD2	UHMWPE/HDPE (50:50)
WAXD	Wide-angle X-ray diffraction analysis
XRD	X-ray diffraction analysis

List of Symbols

Symbol	Description
2θ	X-ray scattering angle
σ	Electric conductivity/Tensile strength
σ_s	Coefficient surface tension
$\sigma(t)$	Average stress in the sample
μ	Viscosity of suspending medium
λ	Wavelength of the X-ray source
ΔH_m	Melt enthalpy
ΔH^0_m	Melt enthalpy of the 100% crystalline polymer
A_S and A_B	Cross-section area of the sample and bars
β	Full-Width Half Maxima (radians)
c^*	Overlap concentration
c_e	Entanglement concentration
c_0	Elastic wave velocity
D	Diffusion coefficient/Pore diameter/Fiber diameter/Crystallites size
D_b	Diameter of the bars
ε	Electric permittivity/elongation at break
ε_0	Permeability of vacuum
$\varepsilon(t)$	Strain rate within the sample
ε_i	Strain due to incident waves
ε_r	Strain due to reflected waves
ε_t	Strain due to transmitted waves
E	Elastic modulus
F_1	Force applied to the sample by the incident bar
F_2	Force applied to the sample by the transmitted bar
g	Gravitational acceleration
G' and G''	Storage and loss modulus
H	Distance between the needle tip to the collector
H_s	Sample thickness
k and K	Boltzmann's constant and Scherrer constant
L	Length of the needle tip

m	Consistency
M_w	Molecular weight of the polymer
n	Power-law index
$[\eta]$	Intrinsic solution viscosity
η_s	Solvent viscosity
η_0	Zero-shear viscosity
η_{sp}	Specific viscosity
N_{av}	Avogadro number
ρ	Mass density of liquid
ρ_p	Densities of polymers
ρ_s	Densities of 1-octanol
p	Differential pressure
Pe	Péclet number
Q	Electrostatic charge
r	Radius of the suspended drop
R	Radius of droplet/Gas constant/Needle radius
$\langle R^2 \rangle^{1/2}$	Root mean squared end-to-end distance
R_a	Arithmetic mean roughness
R_g	Radius of gyration
R_h	Hydrodynamic radius
R_q	RMS roughness
T	Temperature
u_1 and u_2	Incident and transmission bar end displacement
v	Flory's constant
W_w	Weight of the wet mat
W_d	Weight of the dry mat
χ	Flory-Huggins parameter
X_c	Degree of crystallinity
γ	Surface tension of fluid
$\dot{\gamma}$ and $\dot{\gamma}_c$	Shear rate and Critical shear rate
Z	Acoustic impedance of the material

Preamble

Background and motivation

Ballistic protective clothing is required to protect personnel from bullets and fragments. High-performance fibers, namely *p*-aramid-based fibers (Kevlar, Twaron) and ultra-high molecular weight polyethylene (UHMWPE) are specially engineered for ballistic armor, which works as a backbone of today's ballistic armor. However, enhanced sophisticated weapons and war strategy need more excellent threat protection, making present day armor cumbersome. Concerning this area, fabrics are treated with non-Newtonian shear thickening fluid to improve armor flexibility by reducing the number of layers for the same level of protection. Developing lightweight and strong materials for armor have always been an open area for research.

High-performance fibers possess unique properties due to their different base polymer and special fiber manufacturing processes which influence the microscopic structure and chain orientation of fibers. UHMWPE contain an extremely long chain of ethylene molecules which significantly contributes to its strength. In the main ethylene chain, the atoms are bonded with strong covalent bonds, while weak van der Waals bonds are present in the parallel orientation of the molecular chain. Because of its large molecular chain, a long overlap exists among the chain length. Consequently, the cumulative effect of van der Waals bonds is significant over the entire chain, which assists in bearing an enormous shear force between the molecules [1].

UHMWPE fibers produced by gel spinning techniques possess a high tensile strength of around 5 GPa. It is obtained by post-drawing of extruded filament at high temperatures and at different draw ratios [2]. However, it is far from the theoretical tensile strength of 32 GPa and modulus values of 324 GPa of perfect polyethylene crystals of C-C bond strength. Smook et al.[3] suggested that a perfect polyethylene crystal is possible to attain by preparing an extremely thin filament because the actual strength of the fiber is obtained by the lateral bonding between

the molecule [4]. Several methods have been used to make UHMWPE fiber with improved properties by orienting and aligning the molecules [5], [6].

The electrospinning process produces polymeric fibers with diameters varying from nano to several micro-meter ranges, that can possess unique properties like an immensely high surface area to volume ratio and outstanding mechanical properties as compared to larger diameter fibers of the same materials, which motivated this research to fabricate electrospun fibers of UHMWPE. However, the processing of UHMWPE is challenging due to the high melt viscosity and insolubility in common solvents at room temperature. It is only soluble in hydrocarbon solvents such as decalin, p-xylene, paraffin oil, etc., at their theta temperature. Therefore, a high-temperature solution electrospinning process was required to produce ultra-fine fibers of UHMWPE. Moreover, mechanical properties and fibers morphology was controlled by varying spinning processing parameters such as solution rheology, applied voltage, solution concentration, etc. These parameters were needed to be optimized for obtaining the processing window for defect-free uniform fiber of UHMWPE. However, the fully extended orientation of the molecular chain was challenging to achieve only a the single-step electrospinning method due to the high entanglement of UHMWPE chains. This behavior of electrospun fibers created second motivation for improving its performance further. Therefore, a post-processing of electrospun UHMWPE fiber was performed at a high temperature with load, which was further needed to be analyzed for its properties evolvement as compared to Spectra® fibers.

Rheological properties play a significant role in the spinning of fiber solution, which influences the productivity of fibers. High solution viscosity of UHMWPE leads to lower fiber productivity, but it improves by increasing the flowability of the solution by blending with low molecular weight polyethylene, i.e., HDPE. This was the third motivation to increase fiber productivity and determine the morphology of blended fibers, its effect of blending on the

productivity rate, etc. Encapsulation of STF inside an electrospun mat was the fourth motivation for this thesis work. To achieve this task, first, selecting the right nonwoven electrospun mat for STF impregnation, which can absorb a higher amount of STF was done based on fiber surface morphology and pore size distribution inside a mat which was enclosed inside the high temperature stretched electrospun fabric. For evaluation and comparison of properties of electrospun samples, nonwoven felt of UHMWPE was used. To understand ballistic performance of these samples, it was tested at a high strain rate (10^2 - 10^4) in dynamic loading conditions. High strain rate testing was performed using in-house fabricated Split-Hopkinson pressure bars for encapsulated and non-encapsulated electrospun mat and non-woven felt leading to better understanding of its application in future armor technology.

